Supporting Information for:

A structural basis for the regulation of an H-NOX-associated cyclic-di-GMP synthase/phosphodiesterase enzyme by NO-bound H-NOX[†]

Tanaya Lahiri[§], Bowu Luan[§], Daniel P. Raleigh[§#‡], and Elizabeth M. Boon[§#‡]*

[†]This work was supported by the Office of Naval Research grant N00014-10-1-0099 to E.M.B., the National Science Foundation grants CHE-0910771 to E.M.B. and MCB-1330259 to D.P.R., and the National Institutes of Health grant NIH-T32 GM092714 to T.L.

[§]Department of Chemistry, Stony Brook University, Stony Brook, NY, 11794-3400

[‡]Institute of Chemical Biology & Drug Discovery, Stony Brook University, Stony Brook, NY, 11794-3400

[#]Graduate Program in Biochemistry and Structural Biology, Stony Brook University, Stony Brook, NY, 11794-3400

[*]To whom correspondence should be addressed: Elizabeth M. Boon, Department of Chemistry, Stony Brook University, Stony Brook, NY, USA 11790; Tel.: (631) 632-7945; Fax: (631) 632-7960; E-mail: elizabeth.boon@stonybrook.edu

Supporting Table 1: Ligand binding properties and NO off kinetics for the E16K, F17A and E20K mutants of *Sw*H-NOX as compared to WT *Sw*H-NOX. The dissociation rates for the Fe(II)-NO complexes of each *Sw*H-NOX construct were fit to the following equation: $y = y_0 + a_1*(1 - e^{(-b_1*x)}) + a_2*(1-e^{(b_2*x)})$ using Origin 7.0 software. Each experiment was done thrice for error determination.

TABLE S1: Ligand binding properties and NO_{off} kinetics for the E16K, F17A and E20K mutants of *Sw*H-NOX as compared to WT *Sw*H-NOX.

Protein	**Fe(II)**	**Fe(II)-NO**	**Fe(II)-CO**	k_{off}**(NO)** **(x 10^{-4} s^{-1})**	**Ref.**
WT *Sw*H-NOX	431	399	423	15.2 ± 3.50	1
E16K *Sw*H-NOX	431	399	424	7.97 ± 0.06	This study
F17A *Sw*H-NOX	431	398	423	7.45 ± 0.18	This study
E20K *Sw*H-NOX	431	399	423	7.71 ± 0.15	This study

[1]The experiment was performed as previously described (Liu, N.; Xu, Y.; Hossain, S.; Huang, N.; Coursolle, D.; Gralnick, J. A.; Boon, E. M. *Biochemistry* 2012, *51*, 2087).

Supporting Table 2: PPI concentrations used for the standard curve. The last 2 rows show the controls for IPP. As shown for the PPi standard reaction with IPP, the amount of Pi generated in the reaction does not change when the amount of IPP is doubled (10 U/ml and 20 U/ml). This indicates that for the cyclase reactions of *Sw*HaCE with GTP, IPP is not the rate-limiting enzyme, and does not interfere with the enzyme activity.

TABLE S2: Malachite Green Assay; PPi standard curve and IPP control

Reaction	Pi (mM)
0.78 mM PPi + 10 ml IPP	0.00343
1.56 mM PPi + 10 ml IPP	0.00490
3.125 mM PPi + 10 ml IPP	0.01037
6.25 mM PPi + 10 ml IPP	0.04735
12.5 mM PPi + 10 ml IPP	0.06118
25 M mM PPi + 10 ml IPP	0.12349
50 mM PPi + 10 ml IPP	0.27686
25 mM PPi + 10 ml IPP	0.12349
25 mM PPi + 20 ml IPP	0.13303

FIGURE S1: A. Sedimentation equilibrium experiments for the WT *Sw*H-NOX Fe(II)-NO complex conducted using rotor speeds 17,000, 27,000 and 34,000 rpm (g-force of 23,300, 58,700 and 93,000 respectively). The signal at 400 nm was monitored. The molecular weight calculated from HeteroAnalysis is 23.3 kDa. The expected molecular weight for a monomer is 22.5 kDa. **B.** Sedimentation equilibrium experiments for the E16K *Sw*H-NOX Fe(II)-NO complex in solution. The rotor speeds used were same as for WT *Sw*H-NOX in part A. As calculated from HeteroAnalysis, the molecular weight is 23.8 kDa. The expected molecular weight for a monomer Is 22.5 kDa. **C.** Sedimentation equilibrium experiments for the WT *Sw*H-NOX Fe(II)-unligated complex conducted using rotor speeds 17,000, 27,000 and 34,000 rpm (g-force of 23,300, 58,700 and 93,000 respectively). The signal at 430 nm was monitored. The molecular weight calculated from HeteroAnalysis is 23.0 kDa. The expected molecular weight for a monomer is 22.5 kDa. Each experiment was performed in triplicate.

Figure S1. A.

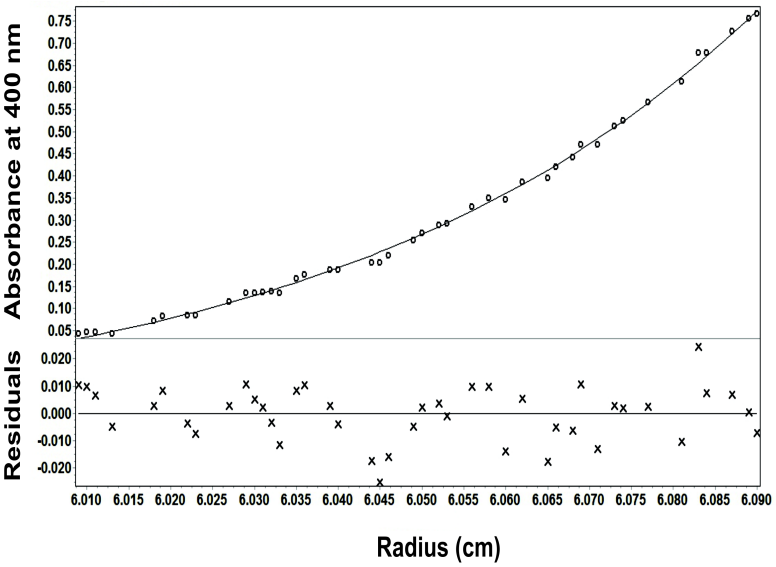

Figure S1. B.

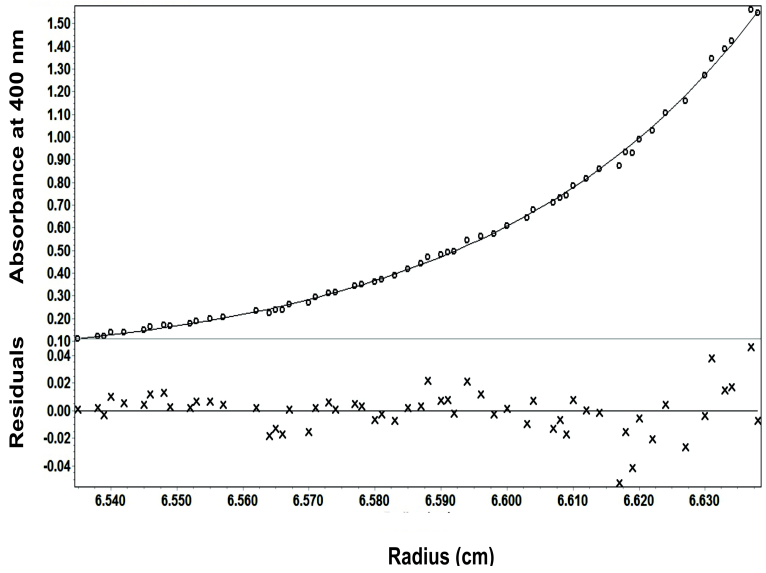

Figure S1. C.

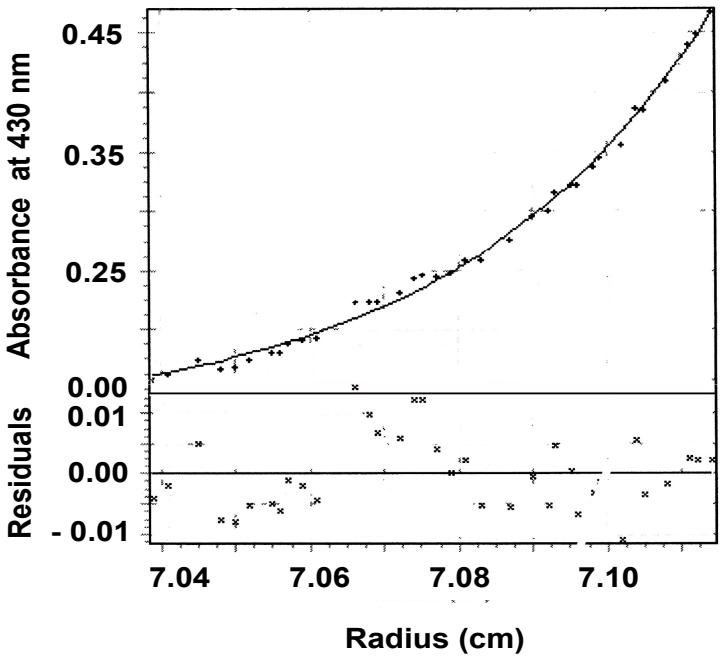
0.45
0.35
0.25
0.00
Absorbance at 430 nm
0.01
0.00
- 0.01
Residuals
7.04
7.06
7.08
7.10
Radius (cm)

FIGURE S2: A. Sedimentation equilibrium experiments for the WT *Sw*H-NOX Fe(II)-unligated complex in association with *Sw*HaCE in solution. Rotor speeds of 9000, 14,000 and 18,000 rpm (g-force of 6500, 15,800 and 26,100 respectively) were used, and the signal at 430 nm was monitored. The molecular weight calculated from HeteroAnalysis is 198.0 kDa, which matches the expected MW of a heterotetrameric complex (197.2 kDa). **B.** Sedimentation equilibrium experiments for the E16K *Sw*H-NOX mutant [as the Fe(II)-NO complex] in association with *Sw*HaCE in solution. Rotor speeds of 9000, 14,000 and 18,000 rpm (g-force of 6500, 15,800 and 26,100 respectively) were used, and the signal at 400 nm was monitored. The molecular weight calculated from HeteroAnalysis is 76 kDa, which does not match the MW of a heterotetrameric complex (197.2 kDa). **C.** Sedimentation equilibrium experiments for the *Sw*WT H-NOX Fe(II)-NO complex by itself in solution. Rotor speeds of 9000, 14,000 and 18,000 rpm (g-force of 6500, 15,800 and 26,100 respectively; these are the optimal rotor speeds for the *Sw*H-NOX + *Sw*HaCE complex) were used, and the signal at 400 nm was followed. The molecular weight calculated from HeteroAnalysis is 75 kDa. The molecular weight of monomeric *Sw*H-NOX is not accurately calculated at the rotor speeds used to analyze the *Sw*H-NOX/*Sw*HaCE complex because higher angular velocities are required for lower molecular weight solutes in order to balance the sedimentation and diffusion forces within the radius of the centrifuge cell. These experiments indicate that E16K *Sw*H-NOX is monomeric in solution with SwHaCE, and therefore the E16K mutation disrupts *Sw*H-NOX-*Sw*HaCE binding. Each experiment was performed in triplicate.

Figure S2. A.

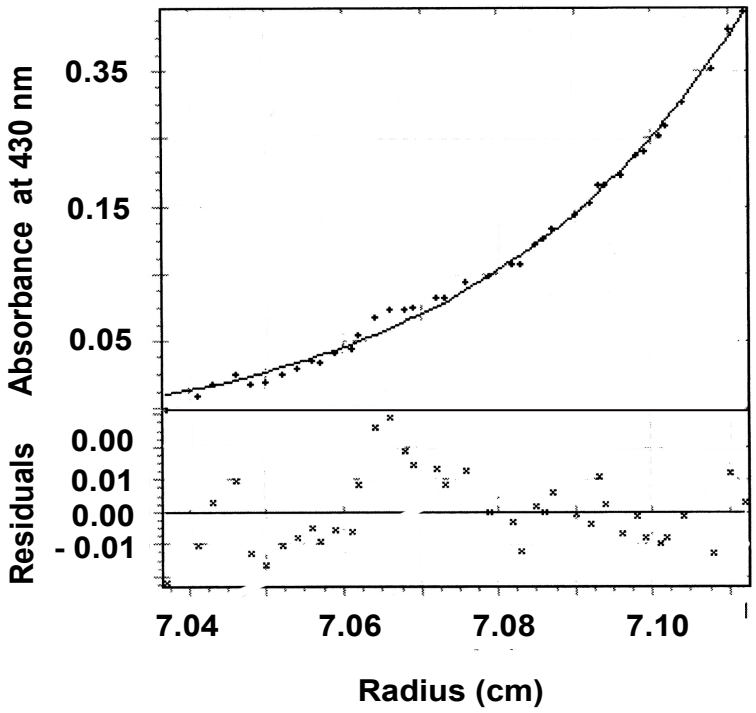

Figure S2. B.

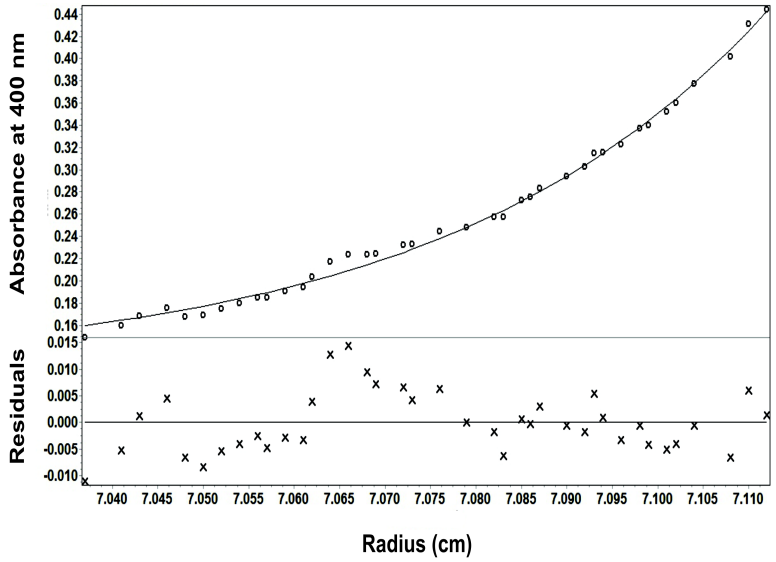

Figure S2. C.

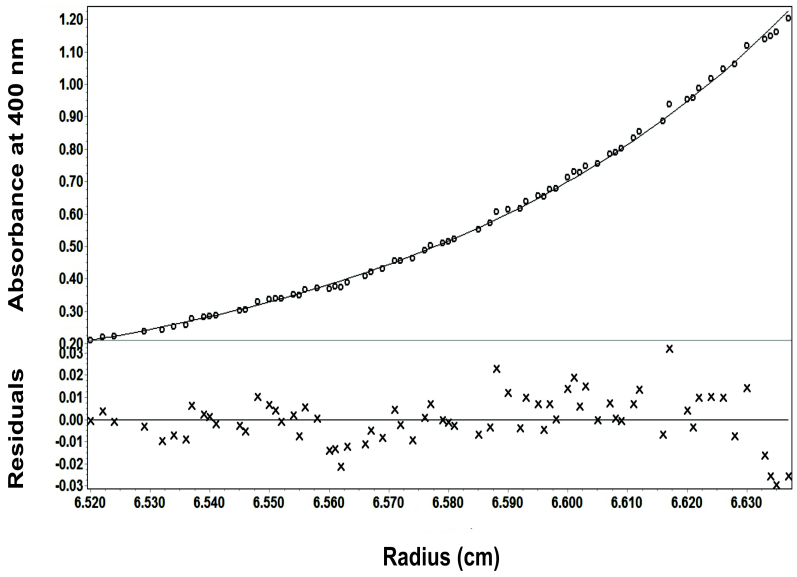
Absorbance at 400 nm
1.20
1.10
1.00
0.90
0.80
0.70
0.60
0.50
0.40
0.30
0.20
Residuals
0.03
0.02
0.01
0.00
-0.01
-0.02
-0.03
6.520
6.530
6.540
6.550
6.560
6.570
6.580
6.590
6.600
6.610
6.620
6.630
Radius (cm)

FIGURE S3: A. A standard curve for PPI was generated for the Malachite Green assay, and IPP was used to cleave the PPI. The concentrations used are listed in table 2. The error bars associated with each data point are smaller than the size of the symbol. **B.** The production of Pi was plotted as a function of increasing *Sw*HaCE concentration. This indicates that *Sw*HaCE is the rate-limiting enzyme, and change in the enzyme concentration changes activity, which is measured by change in the Pi concentration. The error bars for the two data points at the highest concentration are smaller than the size of the symbol.

Figure S3. A.

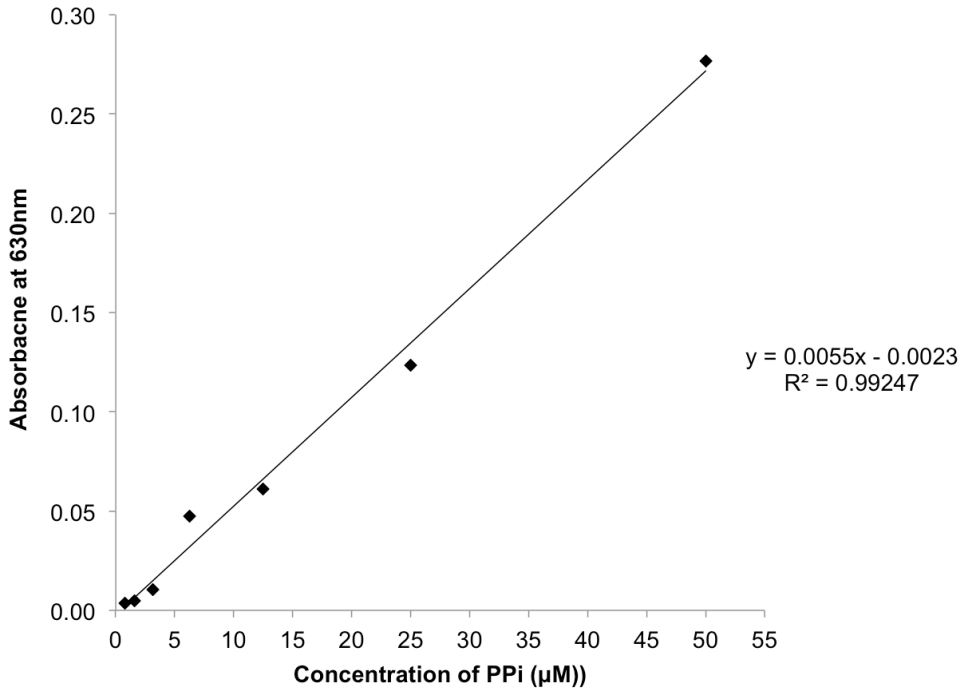

Figure S3. B.

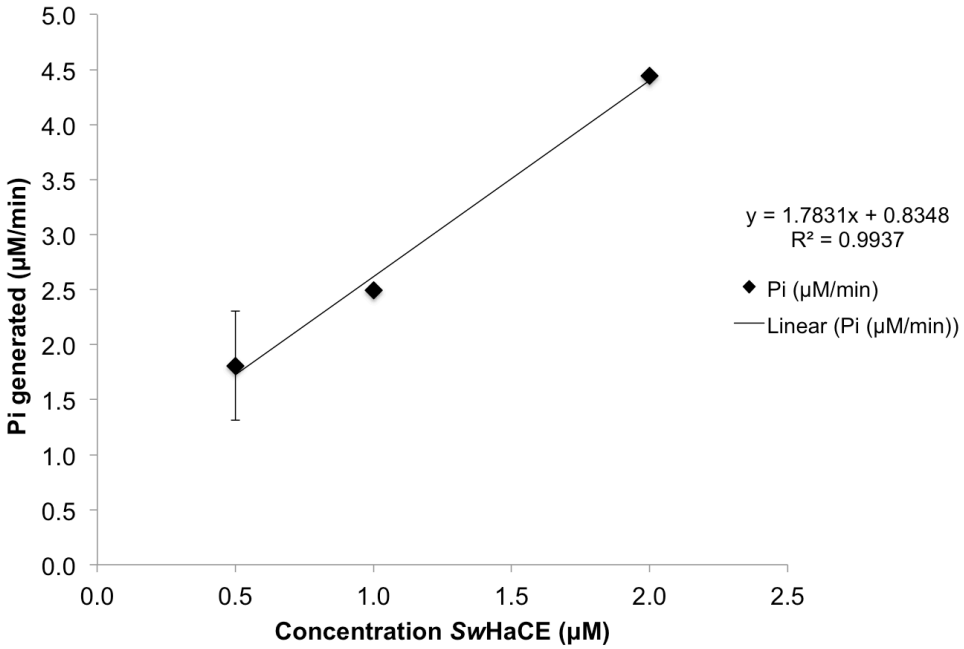
5.0
4.5
4.0
3.5
3.0
2.5
2.0
1.5
1.0
0.5
0.0
Pi generated (µM/min)
0.0
0.5
1.0
1.5
2.0
2.5
Concentration SwHaCE (µM)
y = 1.7831x + 0.8348
R² = 0.9937
Pi (µM/min)
Linear (Pi (µM/min))